Transformations among colloidal semiconductor magic-size clusters

He, Li; Luan, Chaoran; Rowell, Nelson; Zhang, Meng; Chen, Xiaoqin; Yu, Kui

Publisher's version / Version de l'éditeur:
https://doi.org/10.1021/acs.accounts.0c00702
Accounts of Chemical Research, 54, 4, pp. 776-786, 2021-02-03

ACCOUNTS of chemical research

pubs.acs.org/accounts Article

Transformations Among Colloidal Semiconductor Magic-Size Clusters

Published as part of the Accounts of Chemical Research special issue "Transformative Inorganic Nanocrystals".

Li He, Chaoran Luan, Nelson Rowell, Meng Zhang, Xiaoqin Chen,* and Kui Yu*

Cite This: *Acc. Chem. Res.* 2021, 54, 776−786 Read Online

CONSPECTUS: A knowledge of colloidal semiconductor magic-size clusters (MSCs) is essential for understanding how fundamental properties evolve during transformations from individual molecules to semiconductor quantum dots (QDs). Compared to QDs, MSCs display much narrower optical absorption bands; the higher cluster stability gives rise to a narrower size distribution. During the production of binary QDs such as II−VI metal (M) chalcogenide (E) ones, binary ME MSCs observed were interpreted as side products and/or the nuclei of QDs. Prior to the current development of our two-step approach followed by our two-pathway model, it had been extremely challenging to synthesize MSCs as a unique product without the nucleation and growth of QDs. With the two-step approach, we have demonstrated that MSCs can be readily engineered as a sole product at room temperature from a prenucleation stage sample, also called an induction period (IP) sample. It is important that we were able to discover that the evolution of the MSCs follows first-order reaction kinetics behavior. Accordingly, we proposed that a new type of compound, termed as "precursor compounds" (PCs) of MSCs, was produced in an IP sample. Such PCs are optically transparent at the absorption peak positions of their MSC counterparts as well as to longer wavelengths. It is thought that quasi isomerization of a single PC results in the development of one MSC.

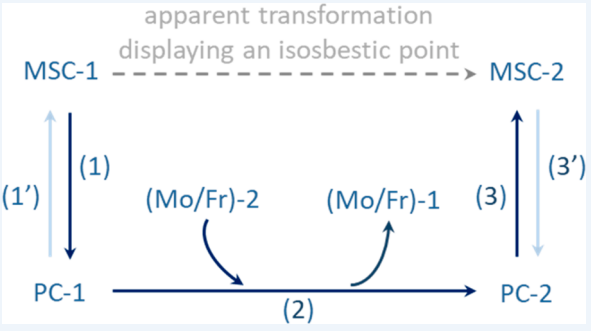

In this Account, we provide an overview of our latest advances regarding the transformations among binary CdE MSCs as well as from binary CdTe to ternary CdTeSe MSCs. Optical absorption spectroscopy has been employed to study these transformations, all of which display well-defined isosbestic points. We have proposed that these MSC to MSC transformations occur via their corresponding PCs, also called immediate PCs. It is reasonable that the as-synthesized PC (in an IP sample) and the immediate PC (in an incubated and/or diluted sample) probably have different configurations. A transformation between two PCs may involve an intermolecular reaction, with either first-order reaction kinetics or a more complicated time profile. A transformation between one immediate PC and its counterpart MSC may contain an intramolecular reaction. The present Account, which addresses the PC-enabled MSC transformations with isosbestic points probed by optical absorption spectroscopy, calls for more experimental and theoretical attention to understand these magic species and their transformation processes more precisely.

KEY REFERENCES

- Zhang, B.; Zhu, T.; Ou, M.; Rowell, N.; Fan, H.; Han, J.; Tan, L.; Dove, M. T.; Ren, Y.; Zuo, X.; Han, S.; Zeng, J.; Yu, K. Thermally-Induced Reversible Structural Isomerization in Colloidal Semiconductor CdS Magic-Size Clusters. *Nat. Commun.* **2018**, *9*, 2499.[1] The thermally induced reversible transformations that occurred between CdS MSC-311 and MSC-322 and displayed isosbestic points at positions between 311 and 322 nm were demonstrated for the first time, with the proposition that CdS MSC-311 and MSC-322 form a pair of quasi isomers. See Table S1 for an explanation of quasi isomers.
- Luan, C. R.; Tang, J. B.; Rowell, N.; Zhang, M.; Huang, W.; Fan, H. S.; Yu, K. Four Types of CdTe Magic-Size Clusters from One Prenucleation Stage Sample at Room Temperature. *J. Phys. Chem. Lett.* **2019**, *10*, 4345−4353.[2] The evolution of four CdTe quasi isomeric MSCs from a single CdTe IP sample was illustrated for the first time, with the hypothesis that the apparent MSC transformations (in the sequence of sMSC-371, sMSC-417, sMSC-448, to dMSC-371 with isosbestic points probed) have occurred through their own counterpart PCs.

Received: October 29, 2020
Published: February 3, 2021

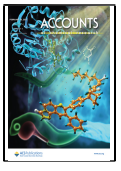

https://dx.doi.org/10.1021/acs.accounts.0c00702
Acc. Chem. Res. 2021, 54, 776−786

- Gao, D.; Hao, X.; Rowell, N.; Kreouzis, T.; Lockwood, D. J.; Han, S.; Fan, H.; Zhang, H.; Zhang, C.; Jiang, Y.; Zeng, J.; Zhang, M.; Yu, K. Formation of Colloidal Alloy Semiconductor CdTeSe Magic-Size Clusters at Room Temperature. *Nat. Commun.* 2019, *10*, 1674.[3] The study reports the first evolution of ternary CdTeSe MSC-399 in a mixture of two binary CdTe and CdSe IP samples at room temperature, together with an intramolecular reaction proposed for the formation of ternary MSCs from their counterpart ternary PCs and with two substitution reactions suggested for the formation of the ternary PC.
- Zhang, H.; Luan, C. R.; Gao, D.; Zhang, M.; Rowell, N.; Willis, M.; Chen, M.; Zeng, J.; Fan, H. S.; Huang, W.; Chen, X.; Yu, K. A Room-Temperature Formation Pathway for CdTeSe Alloy Magic-Size Clusters. *Angew. Chem. Int. Ed.* 2020, *59*, 16943−16952.[4] The first transformation from binary CdTe MSC-371 to ternary CdTeSe MSC-399 which displays an isosbestic point at 380 nm was reported, and a PC-enabled pathway was hypothesized in which the apparent MSC transformation has occurred through their corresponding CdTe PC and CdTeSe PC. Moreover, the formation of the CdTeSe PC involves an intermolecular reaction, namely a substitution reaction of the CdTe PC and CdSe monomer (Mo) or fragment (Fr), instead of that of the CdSe PC and CdTe Mo/Fr.

1. INTRODUCTION

During the past five years, the deliberate, controlled synthesis of colloidal compound semiconductor magic-size clusters (MSCs) has received considerable attention; especially important are those processes not compromised by a simultaneous production of compound semiconductor quantum dots (QDs).[1−27] Originally, the semiconductor MSCs had been observed in the initial stage of the nucleation and growth of the semiconductor QDs.[28,29] With their notable "magic" stability, the MSCs display unique optical properties that are distinctly different from those of the QDs. In samples extracted sequentially from conventional hot-injection and nonhot-injection reaction batches, the MSCs exhibit sharp optical absorption peaking at persistent wavelengths, while the QDs display relatively broad optical absorption with peaks that redshift continuously (due to an increase in size). These spectral and growth differences are closely related to the differences in stability between MSCs and QDs. The magic stability of the MSCs results in a narrow size distribution with only homogeneous spectral line broadening, while the QDs demonstrate both homogeneous and inhomogeneous spectral line broadening together with their optical spectra continuously redshifting.[30,31]

To synthesize semiconductor binary MSCs while excluding binary QDs, a two-step approach was developed and is supported by a two-pathway model.[5] This selective approach consists of two steps, the synthesis of precursor compounds (PCs) of MSCs followed by quasi isomerization of the PC which results in the formation of the counterpart MSC (via an intramolecular reaction). The PC formation occurs in the prenucleation stage of a reaction, so-called the induction period (IP) and takes place at relatively high temperatures (such as above 100 °C). At significantly lower temperatures (such as room temperature), the PC transforms to the MSC when an IP sample is incubated or is diluted in a solvent. This approach, which is based on the use of IP samples, has been demonstrated to be efficient for the production of various types of binary MSCs that are free of QDs, such as CdS,[1,6−8] CdSe,[3,15] and CdTe.[2−4,21,22]

In the two-pathway model,[5] a binary IP sample probably contains binary monomers (Mo), fragments (Fr), as well as PCs, all of which are optically transparent at the absorption peak positions of corresponding MSCs and to longer wavelengths. The existence of the PC in an IP sample has been supported by many experiments. For example, when one CdS IP sample (which was preheated at 180 °C) was dispersed in cyclohexane or toluene (Tol), an evolution of CdS MSC-311 with first-order reaction kinetics was observed.[6] We here point out that the term "immediate precursor" with an abbreviation of IP was used in some of our previous studies,[6,15,21] which we have changed to the present term, "precursor compound" with the PC abbreviation. Matrix-assisted laser desorption/ionization time-of-flight mass spectrometry (MALDI-TOF MS) showed that the CdS PC (in an IP sample) and MSC-311 had similar masses, and we suggested that they form a pair of quasi isomers.[6] When tri-*n*-octylphosphine oxide (TOPO) was added to a CdS IP sample after the formation of the PC, the nucleation and growth of ultrasmall CdS QDs (with enhanced particle yield) took place at temperatures below 160 °C, the underlying cause of which was argued to be TOPO-enhanced fragmentation of the PC.[9] When two binary CdTe and CdSe IP samples (which were respectively preheated at 130 and 140 °C) were mixed at room temperature, ternary CdTeSe MSCs materialized.[3,4]

Here, we collate our latest observations on the transformations among binary CdE MSCs as well as from binary CdTe to ternary CdTeSe MSCs. Optical absorption spectroscopy has been used to follow these transformations, all of which display isosbestic points. For these transformations, we discuss their PC-enabled pathways as shown in Scheme 1. The MSC to MSC transformations are proposed to occur via their corresponding PCs; the MSCs and their PC counterparts are quasi-isomers. The present Account brings a more in-depth understanding of the pathway of the MSC transformations, with the insight gained contributing to the transformation of cluster/nanocrystal synthesis from an empirical art to a science.

2. TRANSFORMATIONS AMONG MSCS

The present Account uses previously reported data with their original accuracy. This section contains four parts, addressing the transformations observed from binary CdS (2.1),[1,8] CdSe (2.2),[15] CdTe MSCs (2.3),[2,21,22] and from binary CdTe to ternary CdTeSe MSCs (2.4).[4] The MSCs are referenced according to the wavelength in nanometers (nm) of their optical absorption peak positions. For example, the two types of CdS MSCs with optical absorption peaking at 311 and 322 nm are referred to as CdS MSC-311 and CdS MSC-322, respectively, while their immediate PCs are labeled as CdS PC-311 and CdS PC-322. For these four types of transformations, their PC-enabled pathways proposed are respectively shown in parts A−D of Scheme 1. As a side note, we have summarized the acronyms that we have used in Table S1, and the key advances in the synthesis of MSCs in Table S2. Also, we recap some evolution of optical absorption in Figure S1, to emphasize the fact that there are different categories of MSCs, while this Account only addresses a special category that transforms from the counterpart PC.

https://dx.doi.org/10.1021/acs.accounts.0c00702
Acc. Chem. Res. 2021, 54, 776−786

Scheme 1. Schematic Drawing of the PC-Enabled Pathways for the MSC Transformations from Binary to Binary CdS (A), CdSe (B), CdTe (C), as well as from Binary CdTe to Ternary CdTeSe (D)[a]

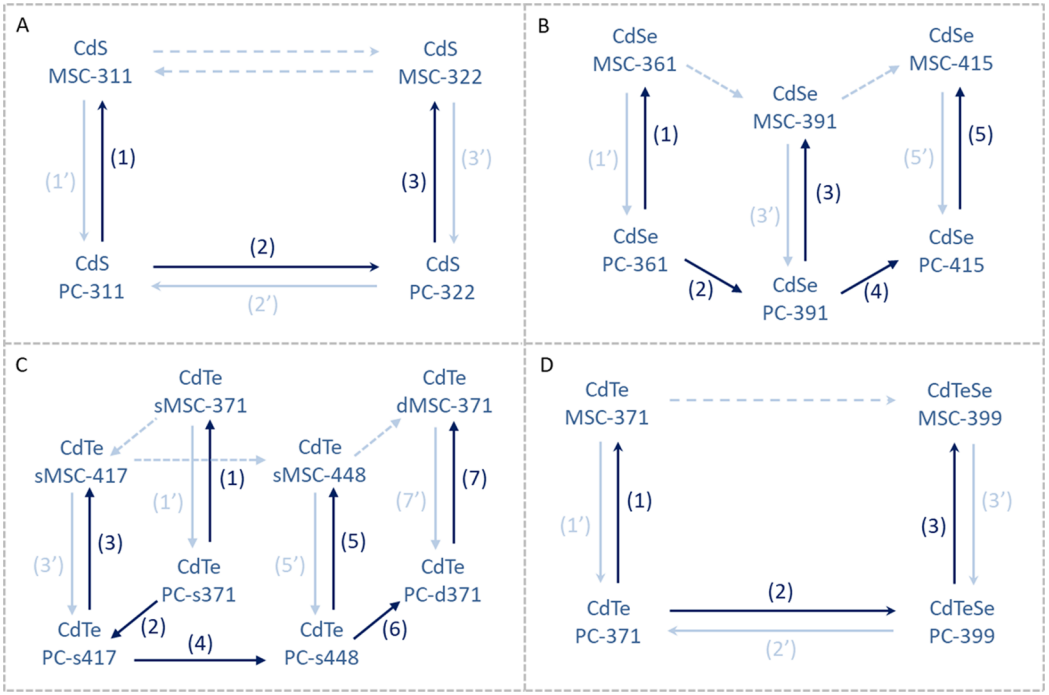

[a]These four types of MSC transformations are respectively discussed in sections 2.1−2.4. The transformations observed from one type of MSCs to another are indicated by dashed-line arrows, while the pathways hypothesized are represented by solid-line arrows. The transformations between a pair of PCs and MSCs contain an intramolecular process, while those between two PCs involve an intermolecular reaction with the breakage of the Cd−E bond and are rate-determining.

The PC to PC transformations in dispersions have been proposed to be rate-determining.[2,4] Importantly, a barrier energy of about 276.8 (in Tol) or 269.3 kJ·mol^{-1} (in cyclohexane) has been obtained for the CdS MSC-311 to MSC-322 transformation, which clearly suggests that the breakage of the Cd−S bond is rate-determining.[1] Accordingly, for a binary to binary PC transformation, we propose a substitution reaction involving the breakage of the Cd−E bond (eq 1), which is similar to that published for the transformation from a binary CdTe PC to a ternary CdTeSe PC (eq 2).[4]

$$\text{CdE PC-1} + \text{CdE(Mo/Fr)-2} \Rightarrow \text{CdE PC-2} + \text{CdE(Mo/Fr)-1} \quad (1)$$

$$\text{CdTe PC} + \text{CdSe Mo/Fr} \Rightarrow \text{CdTeSe PC} + \text{CdTe Mo/Fr} \quad (2)$$

It is evident that through an intra- or intermolecular reaction, respectively, a PC molecule transforms to its counterpart MSC or to another PC (with the breakage of the Cd−E bond as suggested by eqs 1 and 2). For the four types of transformations dealt with in this Account, only the CdS MSC transformations (occurring in Tol or cyclohexane) displayed first-order reaction kinetics. The three remaining types seemed not to follow such a profile, while taking place in mixtures of Tol and octylamine (OTA). It appears, therefore, that there are two distinct types of substitution reactions; to comprehend them, we will be following the schemes of S_N1 and S_N2, which had been respectively proposed for single- and bimolecular nucleophilic substitutions in organic chemistry.[32]

For the PC to PC transformations showing first-order reaction kinetics, we suggest that CdE (Mo/Fr)-1 leaves the substrate CdE PC-1 first, and this process is rate-limiting and is followed by the addition of the substituent CdE (Mo/Fr)-2 that results in the formation of CdE PC-2. For those transformations not following first-order reaction kinetics, the addition of the substituent CdE (Mo/Fr)-2 or CdSe Mo/Fr to the substrate CdE PC-1 or CdTe PC is rate-determining, followed by CdE (Mo/Fr)-1 or CdTe Mo/Fr leaving to form CdE PC-2 or CdTeSe PC, respectively. Table S3 provides a more in-depth discussion of the pathway which has a similarity to either S_N1 or S_N2. Furthermore, the dispersion environment, such as the presence of a protic molecule (primary amines or alcohol), influences the kinetics of the substitution reactions.

2.1. Transformations between CdS MSC-311 and MSC-322

The transformations between CdS MSC-311 and CdS MSC-322 that can be thermally induced have been demonstrated to be reversible and repeatable, while displaying first-order reaction kinetics.[1] Parts A−D of Figure 1 show the optical absorption spectra that were collected in situ when a single dispersion was kept at two different temperatures but in the order of 46 (A), 15 (B), 46 (C), and 15 °C (D). The dispersion was made from a CdS IP sample in cyclohexane. Before the dispersion was set to the first temperature of 46 °C (A), the PC to CdS MSC-311 transformation at room temperature was allowed to complete with no further development of CdS MSC-311. Parts E−H of Figure 1 illustrate the kinetic studies of the transformations which occurred when two Tol dispersions were placed at 52.5 (E and F for the MSC-311 to MSC-322 transformation) and 15.0 °C (G and H for the MSC-322 to MSC-311 transformation), with

https://dx.doi.org/10.1021/acs.accounts.0c00702
Acc. Chem. Res. 2021, 54, 776−786

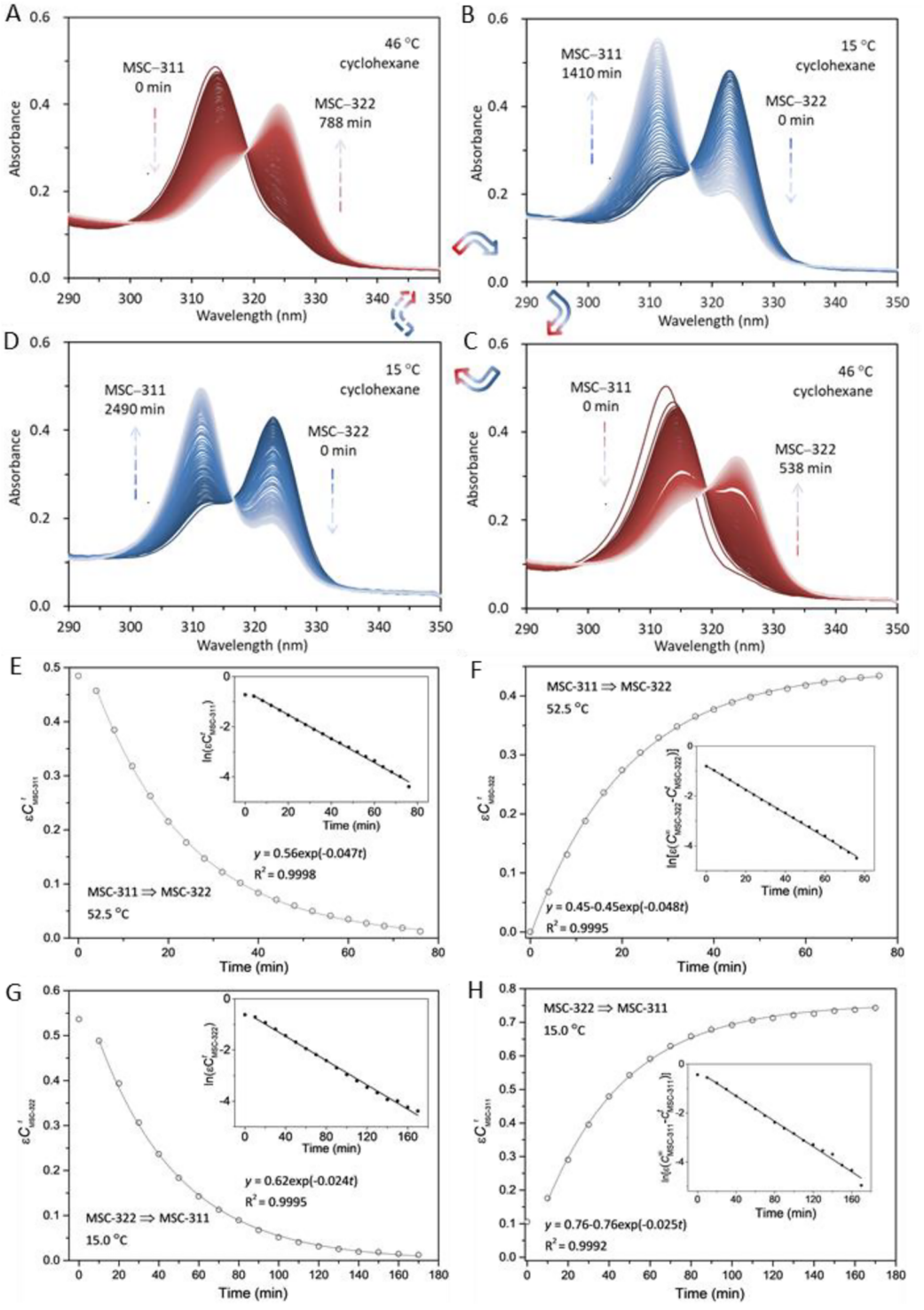

Figure 1. Time-resolved optical absorption spectra (A–D) and kinetic studies (E–H). A CdS IP sample was made from a reaction in octadecene (ODE) of cadmium oleate ($Cd(OA)_2$) and sulfur (S), which was heated at 180 °C for 20 min. Afterward, the IP sample was dispersed in cyclohexane at room temperature. The spectra collected in situ from one dispersion in cyclohexane from 0 to 788 (A), 1410 (B), 538 (C), and 2490 min (D) display well-defined isosbestic points. The transformations from MSC-311 to MSC-322 occurred at 46 °C (A, C), while the reversible ones occurred at 15 °C (B, D). For the former and latter transformations of two dispersions in toluene at 52.5 and 15.0 °C, respectively, the kinetic studies were performed for the reactants (E, G) and products (F, H), with each inset showing the fit to first-order reaction kinetics [Reproduced from ref 1. Copyright 2018 Zhang et al.].

parts E and G for the reactants as well as parts F and H for the products MSC-311.

The transformation from MSC-311 to MSC-322 occurred at relatively high temperatures (46 and 52.5 °C), while the reverse transformation from MSC-322 to MSC-311 was possible at relatively low temperatures (15 °C). The former and latter transformations display well-defined isosbestic points at about 319 and 316 nm, respectively (A–D). See Figure S2 for the two isosbestic points with expanded views. The kinetic study (E–H) suggested that the transformations have first-

https://dx.doi.org/10.1021/acs.accounts.0c00702
Acc. Chem. Res. 2021, 54, 776–786

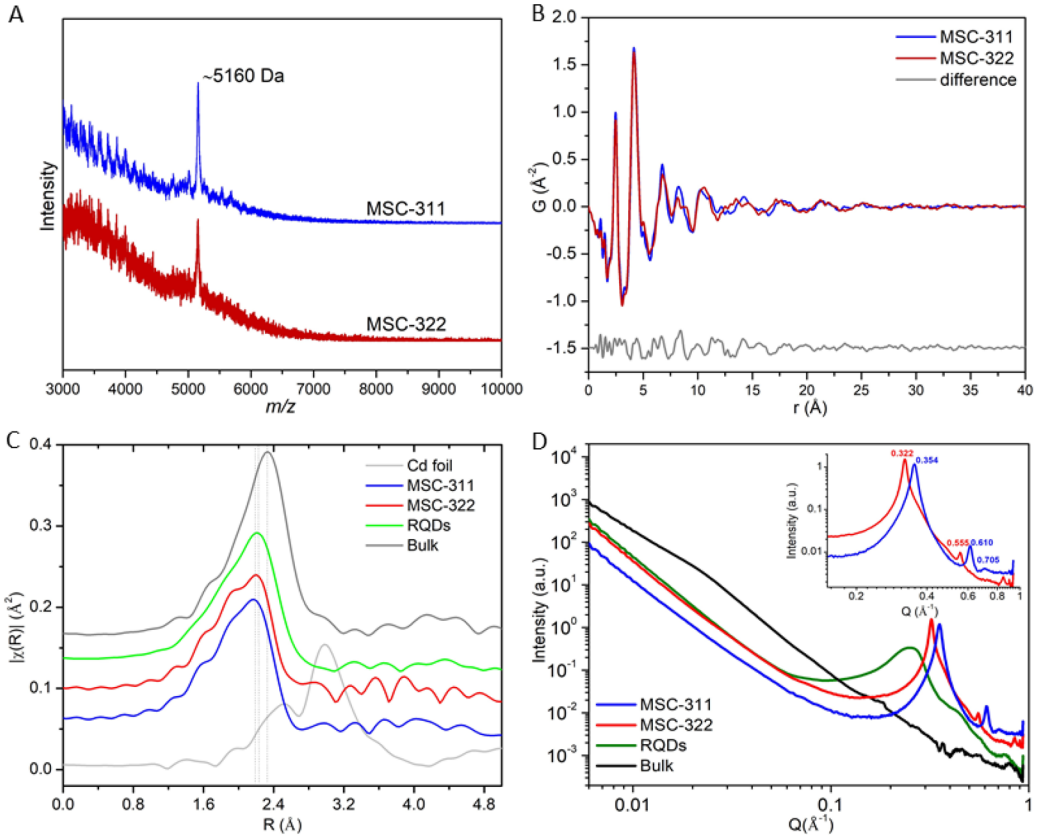

Figure 2. Characterization of CdS MSC-311 (blue traces) and MSC-322 (red traces) with MALDI-TOF MS (A), PDF analysis (B), Cd K-edge X-ray absorption fine structure (XAFS) (C), and small angle X-ray scattering (SAXS) (D). The two types of CdS MSCs form a pair of quasi isomers, with similar masses and local structures but slightly different shapes. [Reproduced from ref 1. Copyright 2018 Zhang et al.].

order reaction kinetics. For the former transformation at 52.5 °C, the rate constant fitted was 0.047 min^{-1} for the reactant MSC-311, which matched well with 0.048 min^{-1} for the product MSC-322. For the latter transformation at 15 °C, it was 0.024 min^{-1} for the reactant MSC-322 and 0.025 min^{-1} for the product MSC-311. Moreover, a barrier energy of about 276.8 (in Tol) or 269.3 kJ·mol^{-1} (in cyclohexane) obtained for the former transformation indicates undoubtedly that the rate-determining step depends on the breakage of the Cd−S bond. See Note S1 for an additional discussion on the rate-determining step. Therefore, we propose that PC-311 and PC-322 are involved for the pathway of the transformations, as shown by part A of Scheme 1. Moreover, the transformations between the two PCs (steps 2 and 2′) are rate-limiting and account for the first-order reaction kinetics observed. As shown by eq 1, the intermolecular reactions which are responsible for the PC to PC transformations involve the breakage of the Cd−S bonds.

We concluded that the four species shown in part A of Scheme 1, CdS PC-311, PC-322, MSC-311, and MSC-322, were members of a group of quasi isomers. As a side note, we hypothesize that other CdS MSCs such as MSC-360 could be included as well.[11,12] When one IP sample was incubated at 4 or 60 °C, the evolution of CdS MSC-311 or MSC-322 was respectively observed. It is evident that relatively low or high temperatures respectively favor the evolution of MSC-311 or MSC-322 (from an original IP sample without dilution). That the two types of CdS MSCs form a pair of quasi isomers is also demonstrated by Figure 2, where MALDI-TOF MS (A) indicates that the two MSCs have similar masses. The MALDI-TOF MS experiments performed for CdS PCs and their counterpart MSCs are summarized in Table S4, with an additional discussion in Note S2. The structural analysis with X-ray total scattering with atomic pair distribution function (PDF) (B) suggests that the two MSCs have similar local structures but slightly different shapes, with almost the same size in the range of 1−2 nm. Clearly, the first two X-ray peaks are much the same; thus, the nearest-neighbor Cd−S, Cd−Cd, and S−S correlations are alike. A noticeable difference is seen in the fourth X-ray peaks. X-ray absorption fine structure (XAFS) (C, the corresponding *k*-space presentation is shown in Figure S3) also illustrates that the two MSCs have similar local structures, while small-angle X-ray scattering (SAXS) (D) demonstrates that the shapes of the two MSCs are slightly different.

In dispersion, the presence of methanol accelerated the evolution of CdS MSC-311 from the PC (in one IP sample) or from MSC-322, with first-order reaction kinetics observed as well.[1,6] With the presence of one α-methyl carboxylic acid (such as $C_{16}H_{33}CH(CH_3)-COOH$ or $C_2H_5CH(CH_3)-COOH$) or diphenylphosphine ($HPPh_2$), the direct production of CdS MSC-311 or MSC-322 could be controlled from the reaction, respectively, which was kept still at a relatively high temperature such as 180 or 100 °C (prior to nucleation and growth of CdS QDs).[7,8] Interestingly, when one α-methyl carboxylic acid and $HPPh_2$ were both present, MSC-311 was produced as the sole product at 100 °C without MSC-322.[8] These experimental results are in agreement with those reported, with regard to the synthesis of MSC-322 via a high concentration approach and the alcohol-assisted transforma-

https://dx.doi.org/10.1021/acs.accounts.0c00702
Acc. Chem. Res. 2021, 54, 776−786

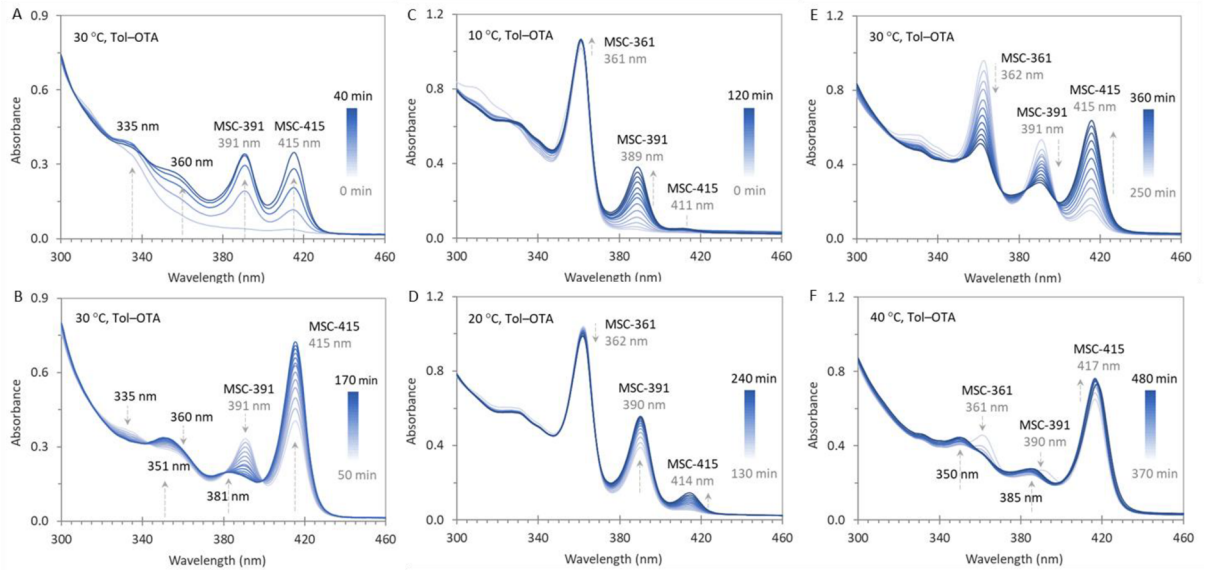

Figure 3. Time-resolved optical absorption spectra collected in situ from one CdSe IP sample. The evolution of various CdSe MSCs includes CdSe MSC-361, MSC-391, and MSC-415. The IP sample was made from a reaction in oleylamine (OLA) of cadmium acetate ($Cd(OAc)_2$) and tri-*n*-octylphosphine selenide (SeTOP), which was heated at 150 °C for 20 min. Two dispersions were prepared at room temperature, each with 300 μL of the IP sample in a mixture of 1.8 mL Tol and 1.2 mL OTA. One dispersion was kept at 30 °C (A and B). The other dispersion underwent a temperature increase from 10 to 40 °C with 120 min at each temperature and a step of 10 °C (C–F). The conditions under which the spectra were collected are indicated, with 0–40 (A) and 50–170 min (B) at 30 °C, 0–120 min at 10 °C (C), 130–240 min at 20 °C (D), 250–360 min at 30 °C (E), and 370–480 min at 40 °C (F). Several well-defined isosbestic points can be seen clearly, such as at 398 nm (B and E). The as-synthesized PC produced in the IP sample evolved at 10 °C to PC-361 (C), but at 30 °C to PC-391 and PC-415 (A) [Reproduced from ref 15. Copyright 2018 American Chemical Society].

tions.[13,14] Collectively, all of the results indicate that with the capability developed to promote or suppress inter-MSC transformations, it is practical to produce one type of MSC as the sole product (with reasonable production yield). For the prenucleation stage, it is estimated that a majority of the Cd and S precursors form PCs which can transform into MSCs.[6−9]

2.2. Evolution of Several CdSe MSCs from a Single IP Sample

Several types of CdSe MSCs, including MSC-361, MSC-391, and MSC-415, evolved from a single CdSe IP sample when it was dispersed in a mixture of Tol and OTA.[15] Figure 3 shows the optical absorption spectra collected in situ from two dispersions made from a CdSe IP sample in a mixture of 1.8 mL Tol and 1.2 mL OTA. See Note S3 for the experimental details and an additional description of the evolution of the optical spectra.

In the two dispersions, MSC-415 remained at the final stage, with a complete disappearance of both MSC-361 and MSC-391 and the appearance of two related peaks at 351 and 381 nm, respectively (B and F). These two absorption peaks were not attributed to be higher-order electronic transitions of MSC-415 but from other species,[15] the assignment of which is different from that previously reported.[33−36] For the transformations from MSC-361, MSC-391, to MSC-415, well-defined isosbestic points appeared at 398 (B), 370, and 398 nm (E), for example. The presence of isosbestic points was reported for CdSe MSC transformations, but without a PC-enabled transformation pathway proposed.[37] As shown by part B of Scheme 1, we propose that the pathway of the CdSe MSC transformations involves their PC counterparts, PC-361, PC-391, and PC-415. Furthermore, it appears that at relatively low temperatures (10 °C, C), an evolution to PC-361 from the as-synthesized PC readily occurred, while at relatively high temperatures (30 °C, A), the preferred evolution was to PC-391 and PC-415.

2.3. Evolution of Four Types of CdTe MSCs from One IP Sample

That the MSC to MSC transformations with isosbestic points involve corresponding PCs has been further supported by the behavior of CdTe MSCs (Figure 4 and part C of Scheme 1).[3] As in cases of CdS and CdSe MSCs, four types of CdTe MSCs, sMSC-371, sMSC-417, sMSC-448, and dMSC-371, were observed to evolve from a single CdTe IP sample. We use "s" or "d" here to distinguish the CdTe MSCs that exhibit a sharp optical absorption singlet or a doublet; for example, the singlet of sMSC-371 (which can be also labeled as MSC-371) peaks at 371 nm, while the doublet of dMSC-371 peaks at 350 and 371 nm. In Figure 4, we show optical absorption spectra which were collected in situ from five dispersions made from one CdTe IP sample. An aliquot (30 μL) of this IP sample was dispersed in 3.0 mL of mixtures of Tol and OTA, which contained the OTA amounts of 0.50 (A), 0.20 (B), 0.05 (C), 0.40 (D–F), and 0.075 mL (G–I).

The development of the four types of CdTe MSCs was closely related to the amount of OTA in dispersion. A relatively large amount OTA (such as 1.50 mL) favored the presence of CdTe sMSC-371 as the sole MSC ensemble without the other three types of CdTe MSCs. When the OTA amount was decreased from 0.50 (A), 0.20 (B), and to 0.05 mL (C), transformations from sMSC-371 to sMSC-417 (during the first 35 min), from sMSC-417 to sMSC-448 (during times from 5 to 110 min), and from sMSC-448 to dMSC-371 (from 25 to 230 min) were observed, respectively. The MSCs, sMSC-417, sMSC-448, and dMSC-371, each developed as nearly a single ensemble after 35 (A), 110 (B), and 230 min (C), respectively. In part A, the sMSC-371 to

https://dx.doi.org/10.1021/acs.accounts.0c00702
Acc. Chem. Res. 2021, 54, 776−786

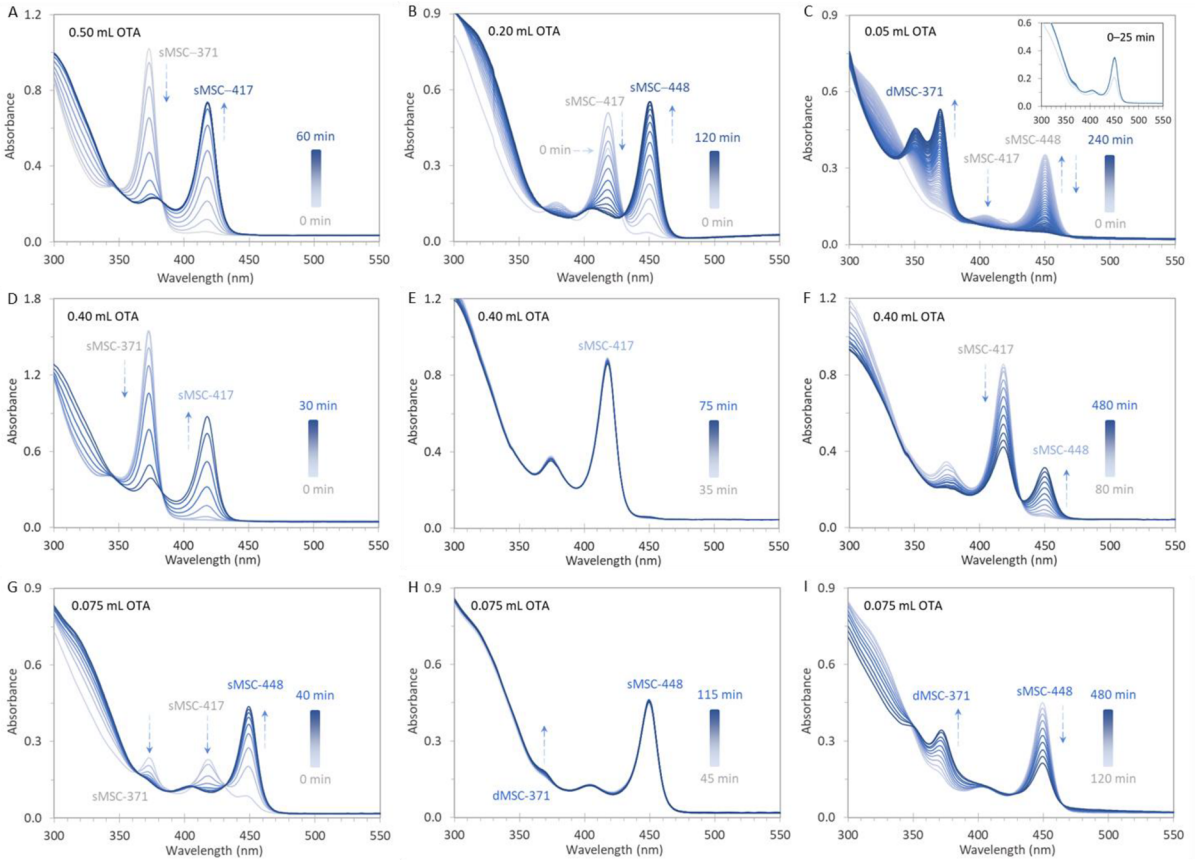

Figure 4. Time-resolved optical absorption spectra collected in situ from a single CdTe IP sample. Four types of CdTe MSCs evolved in a single IP sample, which was made from a reaction in OLA of $Cd(OAc)_2$ and tri-*n*-octylphosphine telluride (TeTOP) heated to 135 °C for 10 min. At room temperature, five dispersions were prepared, each of which had 30 μL of the IP sample in 3.00 mL of mixtures of Tol and OTA with the OTA amount of 0.50 (A), 0.20 (B), 0.05 (C), 0.40 mL (D–F), and 0.075 mL (G–I). In the top panel, the transformations for sMSC-371 to sMSC-417 (A), sMSC-417 to sMSC-448 (B), and sMSC-448 to dMSC-371 (C) are highlighted. The inset in part C shows the relative stability of sMSC-448 from 5 to 25 min. In the middle panel for the transformations from sMSC-371 to sMSC-448 via sMSC-417 (D–F), the relative stability of sMSC-417 from 35 to 75 min is noteworthy (E). In the bottom panel for the development of dMSC-371 via the sequential transformations of sMSC-371, sMSC-417, and sMSC-448 (G–I), the absorption strength of sMSC-448 appeared to be relatively stable from 45 to 115 min (H).The presence of these relatively stable periods is in good agreement with the PC-enabled pathway proposed (as shown by part C of Scheme 1) [Reproduced from ref 2. Copyright 2019 American Chemical Society].

sMSC-417 transformation has a distinct isosbestic point at about 384 nm. In part B, sMSC-417 increased in the first 5 min; afterward, its transformation to sMSC-448 has a definite isosbestic point at about 431 nm. In part C, the strength of sMSC-448 changed little from 5 to 25 min.

The occurrence of a relatively stable stage in the middle of MSC transformations is worthy of notice, which is allowed by the PC-enabled pathway proposed (Scheme 1). Two further examples are shown in the middle and bottom panels of Figure 4. See Note S4 for an additional description of the evolution of the absorption. As indicated in part C of Scheme 1, our model proposes that, similar to the transformations in the CdS and CdSe cases, the apparent transformations for the CdTe MSCs involve their counterpart PCs, PC-s371, PC-s417, PC-s448, and PC-d371. As a side note, the direct evolution of sMSC-448 without the presence of the other three types of CdTe MSCs was also observed, when a CdTe IP sample was dispersed in Tol containing small amounts of alcohol (such as methanol). Interestingly, when certain amounts of primary amine OTA were added, sMSC-371 and sMSC-417 developed, while sMSC-448 changed little. Thus, the methanol-containing dispersion contained an amount of CdTe PCs, which transformed to sMSC-371 and sMSC-417 upon the addition of OTA. Nonetheless, it is not known whether PC-s448 in the methanol-containing dispersion was directly transformed from as-synthesized PCs or from PC-s417 via PC-s371. For the MSC transformations observed, the transformation speed of the two corresponding PCs appeared to be rate-limiting.

2.4. From Binary CdTe MSC-371 to Ternary CdTeSe MSC-399 Transformations

Our PC-enabled pathway model explaining the MSC transformations that display isosbestic points, also accounts for binary to ternary MSC transformations (Figure 5 and part D of Scheme 1).[4] When two IP samples of binary CdTe and CdSe were mixed at room temperature, ternary alloy CdTeSe MSC-399 evolved.[3,4] Figure 5 shows the optical absorption spectra which were collected in situ from five cuvettes with four as-mixed samples (A–D) and one incubated mixture (E and F). See Note S5 for the experimental details and an additional description of the evolution of the optical spectra.

For the two as-mixed samples in the Tol and OTA mixture (A and B), only binary CdTe MSC-371 emerged immediately after dispersion (0 min, red traces) reaching a maximum absorbance strength at 10 (A) and 5 min (B). Subsequently the strength of MSC-371 declined gradually vanishing

https://dx.doi.org/10.1021/acs.accounts.0c00702
Acc. Chem. Res. 2021, 54, 776–786

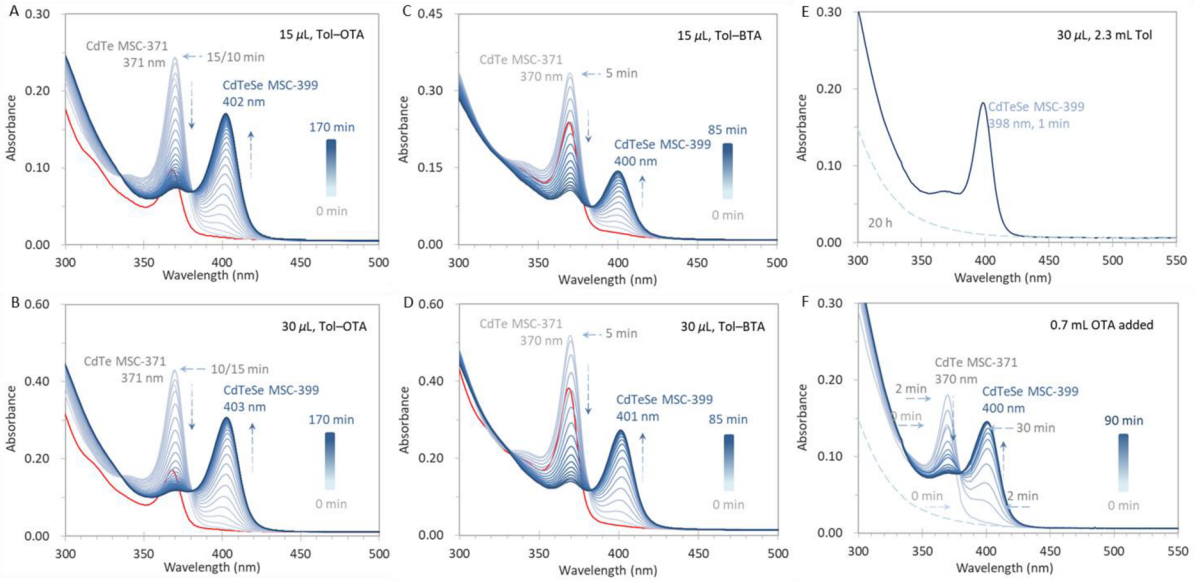

Figure 5. Time-resolved optical absorption spectroscopy for the exploration of the room-temperature evolution of MSCs from mixtures of two CdTe and CdSe IP samples with equal volumes. The CdTe and CdSe IP samples were made from $Cd(OAc)_2$/OLA + TeTOP and $Cd(OAc)_2$/OLA + SeTOP reactions, which were heated for 30 min at, respectively, 130 and 140 °C. 15 μL (A and C) and 30 μL (B and D) portions of as-mixed samples were dispersed in a mixture of 2.0 mL Tol and 1.0 mL OTA (A and B) and of 2.0 mL Tol and 1.0 mL BTA (C and D). The four red traces were collected at 0 min in parts A–D. A 30 μL portion of a mixed sample incubated for 24 h was dispersed in 2.3 mL of Tol (E), to which 0.7 mL OTA was added after a further 20 h (F). The transformations from binary CdTe MSC-371 to ternary CdTeSe MSC-399 display distinct isosbestic points at ~380 nm. The PC-enabled pathway proposed for the binary to ternary MSC transformation is shown in part D of Scheme 1 [Reprinted with permission from ref 4. Copyright 2020 Wiley-VCH Verlag GmbH & Co. KGaA].

completely after 135 (A) and 115 (B) min. Notably from 10 (A) and 5 min (B), the population of CdTeSe MSC-399 started to increase with time reaching a maximum absorbance value of 0.30 at 115 min (A) and of 0.45 at 80 min (B). The two transformations display a distinct isosbestic point at about 380 nm. When BTA replaced OTA (C and D), similar transformations that proceeded faster were observed with a comparable isosbestic point at about 380 nm. The PC-enabled pathway proposed for the binary to ternary transformation is demonstrated in part D of Scheme 1. Here the concept of the formation of binary MSCs via quasi isomerization of their counterpart binary PCs had been generalized to that of ternary MSCs from their ternary PCs.

We proposed a substitution reaction to account for the formation of ternary CdTeSe PCs, as shown by eq 2, which implies that the CdSe PC does not directly participate in the formation of CdTeSe PC-399 but with a fragmentation to CdSe Mo/Fr. Such a notion on the CdSe PC fragmentation concurs with the fact that the evolution of CdSe MSCs was not observed in mixtures of the binary CdTe and CdSe IP samples, which did, however, display CdTe MSC-371 to CdTeSe MSC-399 transformations. Interestingly, the substitution reaction is reversible. The right-to-left reaction of eq 2, namely the ternary CdTeSe PC to binary CdTe PC reaction, had been effectively demonstrated by an incubated sample. After being incubated for 24 h, the sample was dispersed in Tol and CdTeSe MSC-399 developed immediately as a single ensemble without CdTe and/or CdSe MSCs (E, solid trace). After 20 h in the Tol dispersion, CdTeSe MSC-399 disappeared completely (E and F, dashed traces). After the addition of OTA in the Tol dispersion (F), CdTe MSC-371 developed immediately (0 min) and increased at 2 min. The appearance of CdTe MSC-371 suggested the presence of the CdTe PC in the Tol dispersion prior to OTA addition, which was produced from the CdTeSe PC via the right-to-left reaction of eq 2 probably. From 2 to 40 min, CdTe MSC-371 declined continuously and vanished, while CdTeSe MSC-399 kept increasing. Such a transformation from CdTe MSC-371 to CdTeSe MSC-399 also displayed a well-defined isosbestic point at about 380 nm.

For the PC-enabled pathway proposed for the transformation from binary CdTe MSC-371 to ternary CdTeSe MSC-399 (part D of Scheme 1), we would like to point out that when an as-mixed sample is dispersed in a mixture of Tol and amine (OTA or BTA), the CdTe MSC-371 to CdTeSe MSC-399 transformation occurs via steps 1′, 2, and 3 in sequence, for which the rate-determining step is step 2. In an incubated sample, the evolution of CdTeSe MSC-399 appeared to follow steps 2 and 3, with the rate-determining step being step 3.[3]

3. CONCLUSIONS AND PERSPECTIVE

We have reviewed in this Account the transformations among compound semiconductor MSCs, together with an explanation for the transformation pathways which are PC-enabled (Scheme 1). The MSCs addressed are binary CdS, CdSe, CdTe, and ternary CdTeSe, which exhibit sharp optical absorption, while their corresponding PCs are optically transparent at the MSC absorption peaks and longer wavelengths. The transformations from binary to binary or to ternary all show isosbestic points which are located at a wavelength between the absorption peak positions of the starting and ending MSCs. For example, for the transformations from CdS MSC-311 to MSC-322 occurring at relatively high temperatures or from CdS MSC-322 to MSC-311 taking place at relatively low temperatures, the isosbestic points are at about 319 or 316 nm, respectively (Figure 1). Table S5 compares the two published studies on the reversible transformations between CdS MSC-311 and MSC-322.[1,14]

https://dx.doi.org/10.1021/acs.accounts.0c00702
Acc. Chem. Res. 2021, 54, 776–786

These binary MSCs and their corresponding PCs form a group of quasi isomers (Figure 2). For the CdSe MSC-361 to MSC-415 transformations via MSC-391, the isosbestic points are respectively at about 370 and 398 nm (Figure 3); it appears that as-synthesized PCs (in an IP sample) and immediate PCs of one typical type of MSCs have different configurations, with the transformation of the former to PC-361 at a relatively low temperature (10 °C) and to PC-391 and PC-415 at a relatively high temperature (30 °C). For the transformations from CdTe MSC-371 to MSC-417 and from MSC-417 to MSC-448, the isosbestic points are respectively at about 384 and 431 nm; the relatively stable periods for MSC-417 (part E) and MSC-448 (parts C and H) are noteworthy (Figure 4). For the CdTe MSC-371 to CdTeSe MSC-399 transformations, the isosbestic point is at about 380 nm (Figure 5). For the PC-enabled pathways proposed for these MSC transformations (Scheme 1), intra- and intermolecular reactions are respectively involved for those between the PCs and MSCs and between two PCs. For the latter, substitution reactions are proposed, which concern the reactions of PCs and Mo/Fr with the breakage of the Cd−E bond being rate-determining (eqs 1 and 2). We would like to point out that among reported MSCs with one optical absorption singlet, some of their transformations do not have isosbestic points (Figure S1).[16,38−44] Meanwhile, some MSCs display an optical absorption doublet, such as CdSe dMSC-393 and dMSC-460.[17−20,43−47] We are actively studying them and their transformations, although the present Account does not address them. Fascinatingly, the PC concept may apply to III−V semiconductors. For example, InP samples have been produced containing both InP intermediates and QDs; the former displayed a mass of ∼10 kDa, while the latter 60−90 kDa.[48] A possible interpretation of this experimental result would be that InP PCs and/or counterpart MSCs (with a mass of ∼10 kDa) were present in the InP samples; as the reaction proceeded with the nucleation and growth of the InP QDs, the PC/MSC progressively disappeared (Note S2 and Figure S4).

While the synthesis of colloidal semiconductor compound MSCs, including their transformations, has moved forward with more fundamental understanding of their formation pathways, there are still critical challenges, "dark clouds", to be addressed, for example, the composition and configuration of the MSCs and their PCs and as-synthesized PCs, together with the role of alcohol (such as methanol) and primary amines (such as OTA or BTA) in dispersions at a molecular level for transformations from PCs to MSCs or to other PCs via intra- or intermolecular reactions, respectively. It is evident that the surface plays a significant role on the configuration of the PC molecules and MSCs, affecting their electronic structures. It is our hope that more experimental and theoretical attention will be directed to comprehend more precisely the present and novel magic species and processes. In this way, cluster and nanocrystal synthesis can further transform from an empirical art to a science.[32,49]

■ ASSOCIATED CONTENT

Supporting Information

The Supporting Information is available free of charge at https://pubs.acs.org/doi/10.1021/acs.accounts.0c00702.

Four figures, five tables, and five notes, which provide a summary of acronyms used, a literature summary of the key advances in the synthesis of MSCs, and details for the experimental conditions and the evolution of the optical absorption, together with additional explanations of the isosbestic point, rate-determining step, MS, and the pathway proposed for the reactions of eqs 1 and 2 (PDF)

■ AUTHOR INFORMATION

Corresponding Authors

Xiaoqin Chen − *Engineering Research Center in Biomaterials, Sichuan University, Chengdu, Sichuan 610065, People's Republic of China;* orcid.org/0000-0001-7328-2801; Email: xqchen@scu.edu.cn

Kui Yu − *Engineering Research Center in Biomaterials, Sichuan University, Chengdu, Sichuan 610065, People's Republic of China; Institute of Atomic and Molecular Physics, Sichuan University, Chengdu, Sichuan 610065, People's Republic of China;* orcid.org/0000-0003-0349-2680; Email: kuiyu@scu.edu.cn

Authors

Li He − *Engineering Research Center in Biomaterials, Sichuan University, Chengdu, Sichuan 610065, People's Republic of China*

Chaoran Luan − *Department of Ophthalmology, West China School of Medicine, West China Hospital, Sichuan University, Chengdu, Sichuan 610065, People's Republic of China*

Nelson Rowell − *Metrology Research Centre, National Research Council Canada, Ottawa, Ontario K1A 0R6, Canada*

Meng Zhang − *Institute of Atomic and Molecular Physics, Sichuan University, Chengdu, Sichuan 610065, People's Republic of China;* orcid.org/0000-0002-2852-2527

Complete contact information is available at: https://pubs.acs.org/10.1021/acs.accounts.0c00702

Notes

The authors declare no competing financial interest.

Biographies

Li He has earned her bachelor's degree in 2016 from Sichuan University of Science and Engineering and master's degree in 2019 from Southwest University. She joined Sichuan University for her Ph.D. in 2020, supervised by Prof Kui Yu.

Chaoran Luan has earned his Ph.D. in 2020 under the supervision of Prof Kui Yu, and started his postdoctoral fellowship in West China Hospital.

Nelson Rowell obtained his Ph.D. from the University of Toronto and is working as a Principal Research Officer at the National Research Council of Canada.

Meng Zhang earned his Ph.D. from University of Montreal (Canada) in 2017 and started to work with Prof Kui Yu as a postdoctoral fellow the same year, being on the way to a promotion to Associate Professor at Sichuan University.

Xiaoqin Chen earned her Ph.D. in 2017 from Sichuan University and started her postdoctoral fellowship with Prof Kui Yu.

Kui Yu earned her Ph.D. from McGill University. After two postdoctoral fellowships, she joined the National Research Council of Canada as an Assistant Research Officer and was promoted to a Senior Research Officer via an Associate Research Officer. Afterwards, she moved back to her hometown Chengdu, focusing on in-depth

https://dx.doi.org/10.1021/acs.accounts.0c00702
Acc. Chem. Res. 2021, 54, 776−786

fundamental understanding of the evolution of colloidal semiconductor clusters and nanocrystals.

■ ACKNOWLEDGMENTS

K.Y. is profoundly grateful to all her past and current students and co-workers, who have contributed intellectually and technically over the past 15 years to the discovery of MSCs. K.Y. thanks the National Natural Science Foundation of China (NSFC) 21773162, the Science and Technology Department of Sichuan Province for Application-Oriented Fundamental Research Program 2020YJ0326, the State Key Laboratory of Polymer Materials Engineering of Sichuan University for Grant No. sklpme2020-2-09, and the Open Project of Key State Laboratory for Supramolecular Structures and Materials of Jilin University for SKLSSM 202035. X.C. is grateful to the National Natural Science Foundation of China (NSFC), 32000934. We are in debt to Mr. Jinming Zhu for a helpful, in-depth discussion about S_N1 and S_N2 which aided us in understanding the intermolecular reactions involved in the PC to PC transformations.

■ REFERENCES

(1) Zhang, B.; Zhu, T.; Ou, M.; Rowell, N.; Fan, H.; Han, J.; Tan, L.; Dove, M. T.; Ren, Y.; Zuo, X.; Han, S.; Zeng, J.; Yu, K. Thermally-Induced Reversible Structural Isomerization in Colloidal Semiconductor CdS Magic-Size Clusters. *Nat. Commun.* **2018**, *9*, 2499.

(2) Luan, C.; Tang, J.; Rowell, N.; Zhang, M.; Huang, W.; Fan, H.; Yu, K. Four Types of CdTe Magic-Size Clusters from One Prenucleation Stage Sample at Room Temperature. *J. Phys. Chem. Lett.* **2019**, *10*, 4345−4353.

(3) Gao, D.; Hao, X.; Rowell, N.; Kreouzis, T.; Lockwood, D. J.; Han, S.; Fan, H.; Zhang, H.; Zhang, C.; Jiang, Y.; Zeng, J.; Zhang, M.; Yu, K. Formation of Colloidal Alloy Semiconductor CdTeSe Magic-Size Clusters at Room Temperature. *Nat. Commun.* **2019**, *10*, 1674.

(4) Zhang, H.; Luan, C.; Gao, D.; Zhang, M.; Rowell, N.; Willis, M.; Chen, M.; Zeng, J.; Fan, H.; Huang, W.; Chen, X.; Yu, K. A Room-Temperature Formation Pathway for CdTeSe Alloy Magic-Size Clusters. *Angew. Chem., Int. Ed.* **2020**, *59*, 16943−16952.

(5) Palencia, C.; Yu, K.; Boldt, K. The Future of Colloidal Semiconductor Magic-Size Clusters. *ACS Nano* **2020**, *14*, 1227−1235.

(6) Zhu, T.; Zhang, B.; Zhang, J.; Lu, J.; Fan, H.; Rowell, N.; Ripmeester, J. A.; Han, S.; Yu, K. Two-Step Nucleation of CdS Magic-Size Nanocluster MSC-311. *Chem. Mater.* **2017**, *29*, 5727−5735.

(7) Zhang, J.; Hao, X.; Rowell, N.; Kreouzis, T.; Han, S.; Fan, H.; Zhang, C.; Hu, C.; Zhang, M.; Yu, K. Individual Pathways in the Formation of Magic-Size Clusters and Conventional Quantum Dots. *J. Phys. Chem. Lett.* **2018**, *9*, 3660−3666.

(8) Zhang, J.; Li, L.; Rowell, N.; Kreouzis, T.; Willis, M.; Fan, H.; Zhang, C.; Huang, W.; Zhang, M.; Yu, K. One-Step Approach to Single-Ensemble CdS Magic-Size Clusters with Enhanced Production Yields. *J. Phys. Chem. Lett.* **2019**, *10*, 2725−2732.

(9) Li, L.; Zhang, J.; Zhang, M.; Rowell, N.; Zhang, C.; Wang, S.; Lu, J.; Fan, H.; Huang, W.; Chen, X.; Yu, K. Fragmentation of Magic-Size Cluster Precursor Compounds into Ultrasmall CdS Quantum Dots with Enhanced Particle Yield at Low Temperatures. *Angew. Chem., Int. Ed.* **2020**, *59*, 12013−12021.

(10) Wan, W.; Zhang, M.; Zhao, M.; Rowell, N.; Zhang, C.; Wang, S.; Kreouzis, T.; Fan, H.; Huang, W.; Yu, K. Room-Temperature Formation of CdS Magic-Size Clusters in Aqueous Solutions Assisted by Primary Amines. *Nat. Commun.* **2020**, *11*, 4199.

(11) Tang, J. B.; Hui, J.; Zhang, M.; Fan, H. S.; Rowell, N.; Huang, W.; Jiang, Y. N.; Chen, X. Q.; Yu, K. CdS Magic-Size Clusters Exhibiting One Sharp Ultraviolet Absorption Singlet Peaking at 361 nm. *Nano Res.* **2019**, *12*, 1437−1444.

(12) Nevers, D. R.; Williamson, C. B.; Hanrath, T.; Robinson, R. D. Surface Chemistry of Cadmium Sulfide Magic-Sized Clusters: A Window into Ligand-Nanoparticle Interactions. *Chem. Commun.* **2017**, *53*, 2866−2869.

(13) Nevers, D. R.; Williamson, C. B.; Savitzky, B. H.; Hadar, I.; Banin, U.; Kourkoutis, L. F.; Hanrath, T.; Robinson, R. D. Mesophase Formation Stabilizes High-Purity Magic-Sized Clusters. *J. Am. Chem. Soc.* **2018**, *140*, 3652−3662.

(14) Williamson, C. B.; Nevers, D. R.; Nelson, A.; Hadar, I.; Banin, U.; Hanrath, T.; Robinson, R. D. Chemically Reversible Isomerization of Inorganic Clusters. *Science* **2019**, *363*, 731−735.

(15) Zhu, D.; Hui, J.; Rowell, N.; Liu, Y.; Chen, Q. Y.; Steegemans, T.; Fan, H.; Zhang, M.; Yu, K. Interpreting the Ultraviolet Absorption in the Spectrum of 415 nm-Bandgap CdSe Magic-Size Clusters. *J. Phys. Chem. Lett.* **2018**, *9*, 2818−2824.

(16) Li, L.; Zhang, M.; Rowell, N.; Kreouzis, T.; Fan, H.; Yu, Q.; Huang, W.; Chen, X.; Yu, K. Identifying Clusters and/or Small-Size Quantum Dots in Colloidal CdSe Ensembles with Optical Spectroscopy. *J. Phys. Chem. Lett.* **2019**, *10*, 6399−6408.

(17) Liu, Y.; Willis, M.; Rowell, N.; Luo, W.; Fan, H.; Han, S.; Yu, K. Effect of Small Molecule Additives in the Prenucleation Stage of Semiconductor CdSe Quantum Dots. *J. Phys. Chem. Lett.* **2018**, *9*, 6356−6363.

(18) Liu, Y.; Zhang, B.; Fan, H.; Rowell, N.; Willis, M.; Zheng, X.; Che, R.; Han, S.; Yu, K. Colloidal CdSe 0-Dimension Nanocrystals and Their Self-Assembled 2-Dimension Structures. *Chem. Mater.* **2018**, *30*, 1575−1584.

(19) Liu, Y.; Rowell, N.; Willis, M.; Zhang, M.; Wang, S.; Fan, H.; Huang, W.; Chen, X.; Yu, K. Photoluminescent Colloidal Nanohelices Self-Assembled from CdSe Magic-Size Clusters via Nanoplatelets. *J. Phys. Chem. Lett.* **2019**, *10*, 2794−2801.

(20) Chen, M.; Luan, C.; Zhang, M.; Rowell, N.; Willis, M.; Zhang, C.; Wang, S.; Zhu, X.; Fan, H.; Huang, W.; Yu, K.; Liang, B. Evolution of CdTe Magic-Size Clusters with Single Absorption Doublet Assisted by Adding Small Molecules during Prenucleation. *J. Phys. Chem. Lett.* **2020**, *11*, 2230−2240.

(21) Liu, M.; Wang, K.; Wang, L.; Han, S.; Fan, H.; Rowell, N.; Ripmeester, J. A.; Renoud, R.; Bian, F.; Zeng, J.; Yu, K. Probing Intermediates of the Induction Period Prior to Nucleation and Growth of Semiconductor Quantum Dots. *Nat. Commun.* **2017**, *8*, 15467.

(22) Luan, C.; Gokcinar, O. O.; Rowell, N.; Kreouzis, T.; Han, S.; Zhang, M.; Fan, H.; Yu, K. Evolution of Two Types of CdTe Magic-Size Clusters from a Single Induction Period Sample. *J. Phys. Chem. Lett.* **2018**, *9*, 5288−5295.

(23) Liu, S.; Yu, Q.; Zhang, C.; Zhang, M.; Rowell, N.; Fan, H.; Huang, W.; Yu, K.; Liang, B. Transformation of ZnS Precursor Compounds to Magic-Size Clusters Exhibiting Optical Absorption Peaking at 269 nm. *J. Phys. Chem. Lett.* **2020**, *11*, 75−82.

(24) Wang, L.; Hui, J.; Tang, J.; Rowell, N.; Zhang, B.; Zhu, T.; Zhang, M.; Hao, X.; Fan, H.; Zeng, J.; Han, S.; Yu, K. Precursor Self-Assembly Identified as a General Pathway for Colloidal Semiconductor Magic-Size Clusters. *Adv. Sci.* **2018**, *5*, 1800632.

(25) Yang, J.; Muckel, F.; Baek, W.; Fainblat, R.; Chang, H.; Bacher, G.; Hyeon, T. Chemical Synthesis, Doping, and Transformation of Magic-Sized Semiconductor Alloy Nanoclusters. *J. Am. Chem. Soc.* **2017**, *139*, 6761−6770.

(26) Kwon, Y.; Oh, J.; Lee, E.; Lee, S. H.; Agnes, A.; Bang, G.; Kim, J.; Kim, D.; Kim, S. Evolution from Unimolecular to Colloidal-Quantum-Dot-Like Character in Chlorine or Zinc Incorporated InP Magic Size Clusters. *Nat. Commun.* **2020**, *11*, 3127.

(27) Wang, F.; Wang, Y.; Liu, Y. H.; Morrison, P. J.; Loomis, R. A.; Buhro, W. E. Two-Dimensional Semiconductor Nanocrystals: Properties, Templated Formation, and Magic-Size Nanocluster Intermediates. *Acc. Chem. Res.* **2015**, *48*, 13−21.

(28) Peng, Z. A.; Peng, X. Nearly Monodisperse and Shape-Controlled CdSe Nanocrystals via Alternative Routes: Nucleation and Growth. *J. Am. Chem. Soc.* **2002**, *124*, 3343−3353.

https://dx.doi.org/10.1021/acs.accounts.0c00702
Acc. Chem. Res. 2021, 54, 776−786

(29) Pan, D.; Ji, X.; An, L.; Lu, Y. Observation of Nucleation and Growth of CdS Nanocrystals in a Two-Phase System. *Chem. Mater.* **2008**, *20*, 3560−3566.
(30) Empedocles, B. S. A.; Neuhauser, R.; Shimizu, K.; Bawendi, M. G. Photoluminescence from Single Semiconductor Nanostructures. *Adv. Mater.* **1999**, *11*, 1243−1256.
(31) Cui, J.; Beyler, A. P.; Marshall, L. F.; Chen, O.; Harris, D. K.; Wanger, D. D.; Brokmann, X.; Bawendi, M. G. Direct Probe of Spectral Inhomogeneity Reveals Synthetic Tunability of Single-Nanocrystal Spectral Linewidths. *Nat. Chem.* **2013**, *5*, 602−606.
(32) Wang, F.; Richards, V. N.; Shields, S. P.; Buhro, W. E. Kinetics and Mechanisms of Aggregative Nanocrystal Growth. *Chem. Mater.* **2014**, *26*, 5−21.
(33) Kasuya, A.; Sivamohan, R.; Barnakov, Y. A.; Dmitruk, I. M.; Nirasawa, T.; Romanyuk, V. R.; Kumar, V.; Mamykin, S. V.; Tohji, K.; Jeyadevan, B.; Shinoda, K.; Kudo, T.; Terasaki, O.; Liu, Z.; Belosludov, R. V.; Sundararajan, V.; Kawazoe, Y. Ultra-Stable Nanoparticles of CdSe Revealed from Mass Spectrometry. *Nat. Mater.* **2004**, *3*, 99−102.
(34) Cossairt, B. M.; Owen, J. S. CdSe Clusters: At the Interface of Small Molecules and Quantum Dots. *Chem. Mater.* **2011**, *23*, 3114−3119.
(35) Newton, J. C.; Ramasamy, K.; Mandal, M.; Joshi, G. K.; Kumbhar, A.; Sardar, R. Low-Temperature Synthesis of Magic-Sized CdSe Nanoclusters: Influence of Ligands on Nanocluster Growth and Photophysical Properties. *J. Phys. Chem. C* **2012**, *116*, 4380−4389.
(36) Dolai, S.; Nimmala, P. R.; Mandal, M.; Muhoberac, B. B.; Dria, K.; Dass, A.; Sardar, R. Isolation of Bright Blue Light-Emitting CdSe Nanocrystals with 6.5 kDa Core in Gram Scale: High Photoluminescence Efficiency Controlled by Surface Ligand Chemistry. *Chem. Mater.* **2014**, *26*, 1278−1285.
(37) Beecher, A. N.; Yang, X.; Palmer, J. H.; LaGrassa, A. L.; Juhas, P.; Billinge, S. J.; Owen, J. S. Atomic Structures and Gram Scale Synthesis of Three Tetrahedral Quantum Dots. *J. Am. Chem. Soc.* **2014**, *136*, 10645−10653.
(38) Kudera, S.; Zanella, M.; Giannini, C.; Rizzo, A.; Li, Y.; Gigli, G.; Cingolani, R.; Ciccarella, G.; Spahl, W.; Parak, W. J.; Manna, L. Sequential Growth of Magic-Size CdSe Nanocrystals. *Adv. Mater.* **2007**, *19*, 548−552.
(39) Sun, M.; Yang, X. Phosphine-Free Synthesis of High-Quality CdSe Nanocrystals in Noncoordination Solvents: "Activating Agent" and "Nucleating Agent" Controlled Nucleation and Growth. *J. Phys. Chem. C* **2009**, *113*, 8701−8709.
(40) Dukes, A. D.; McBride, J. R.; Rosenthal, S. J. Synthesis of Magic-Sized CdSe and CdTe Nanocrystals with Diisooctylphosphinic Acid. *Chem. Mater.* **2010**, *22*, 6402−6408.
(41) Evans, C. M.; Love, A. M.; Weiss, E. A. Surfactant-Controlled Polymerization of Semiconductor Clusters to Quantum Dots Through Competing Step-Growth and Living Chain-Growth Mechanisms. *J. Am. Chem. Soc.* **2012**, *134*, 17298−17305.
(42) Yu, K.; Ouyang, J.; Leek, D. M. In Situ Observation of PbSe Nucleation and Growth of Magic-Sized Nanoclusters and Regular Nanocrystals. *Small* **2011**, *7*, 2250−2262.
(43) Yu, K.; Hu, M. Z.; Wang, R.; Piolet, M. L.; Zaman, M. B.; Wu, X.; Leek, D. M.; Tao, Y.; Wilkinson, D.; Li, C.; Frotey, M. Thermodynamic Equilibrium-Driven Formation of Single-Sized Nanocrystals: Reaction Media Tuning CdSe Magic-Sized versus Regular Quantum Dots. *J. Phys. Chem. C* **2010**, *114*, 3329−3339.
(44) Yu, K. CdSe Magic-Sized Nuclei, Magic-Sized Nanoclusters and Regular Nanocrystals: Monomer Effects on Nucleation and Growth. *Adv. Mater.* **2012**, *24*, 1123−1132.
(45) Ouyang, J.; Zaman, B. M.; Yan, F.; Johnston, D.; Li, G.; Wu, X.; Leek, D.; Ratcliffe, C. I.; Ripmeester, J. A.; Yu, K. Multiple Families of Magic-Sized CdSe Nanocrystals with Strong Bandgap Photoluminescence via Non-Injection One-Pot Syntheses. *J. Phys. Chem. C* **2008**, *112*, 13805−13811.
(46) Wang, R.; Ouyang, J.; Nikolaus, S.; Brestaz, L.; Zaman, B. M.; Wu, X.; Leek, D.; Ratcliffe, C. I.; Yu, K. Single-Sized Colloidal CdTe Nanocrystals with Strong Bandgap Photoluminescence. *Chem. Commun.* **2009**, 962−964.
(47) Wang, R.; Calvignanello, O.; Ratcliffe, C. I.; Wu, X.; Leek, D. M.; Zaman, M. B.; Kingston, D.; Ripmeester, J. A.; Yu, K. Homogeneously-Alloyed CdTeSe Single-Sized Nanocrystals with Bandgap Photoluminescence. *J. Phys. Chem. C* **2009**, *113*, 3402−3408.
(48) Xie, L.; Shen, Y.; Franke, D.; Sebastian, V.; Bawendi, M. G.; Jensen, K. F. Characterization of Indium Phosphide Quantum Dot Growth Intermediates Using MALDI-TOF Mass Spectrometry. *J. Am. Chem. Soc.* **2016**, *138*, 13469−13472.
(49) Liu, Z. Room-Temperature Synthesis and Formation Pathway of CdTeSe Alloy Magic-Size Clusters. *Acta Phys.-Chim. Sin.* **2020**, *37*, 2008014.

https://dx.doi.org/10.1021/acs.accounts.0c00702
Acc. Chem. Res. 2021, 54, 776−786